Available online at www.sciencedirect.com

ScienceDirect

Current Opinion in
Colloid & Interface Science

Peptide meets membrane: Investigating peptide-lipid interactions using small-angle scattering techniques

Josefine Eilsø Nielsen[1], Vladimir Rosenov Koynarev[1] and Reidar Lund[1,2]

Abstract

Peptide–lipid interactions play an important role in defining the mode of action of drugs and the molecular mechanism associated with many diseases. Model membranes consisting of simple lipid mixtures mimicking real cell membranes can provide insight into the structural and dynamic aspects associated with these interactions. Small-angle scattering techniques based on X-rays and neutrons (SAXS/SANS) allow *in situ* determination of peptide partition and structural changes in lipid bilayers in vesicles with relatively high resolution between 1-100 nm. With advanced instrumentation, time-resolved SANS/SAXS can be used to track equilibrium and nonequilibrium processes such as lipid transport and morphological transitions to time scales down to a millisecond. In this review, we provide an overview of recent advances in the understanding of complex peptide–lipid membrane interactions using SAXS/SANS methods and model lipid membrane unilamellar vesicles. Particular attention will be given to the data analysis, possible pitfalls, and how to extract quantitative information using these techniques.

Addresses

[1] Department of Chemistry, University of Oslo, Postboks 1033, Blindern, Oslo, 0315, Norway

[2] Hylleraas Centre for Quantum Molecular Sciences, University of Oslo, Postboks 1033, Blindern, Oslo, 0315, Norway

Corresponding author: Lund, Reidar (reidar.lund@kjemi.uio.no)

Current Opinion in Colloid & Interface Science 2023, **66**:101709

This review comes from a themed issue on **Biological (bio-inspired) Colloids and Interfaces (2023)**

Edited by **Martin Malmsten** and **Stefan Zauscher**

For complete overview about the section, refer Biological (bio-inspired) Colloids and Interfaces (2023)

https://doi.org/10.1016/j.cocis.2023.101709

Keywords

Lipid membranes, Surface active peptides, Antimicrobial peptides, Amyloids, Small-angle X-ray scattering (SAXS), Small-angle neutron scattering (SANS).

Introduction

A large group of biologically relevant peptides are considered to be surface active, interacting with lipid cell membranes of either host cells. Examples include amyloid peptides linked to human diseases like Alzheimer's disease and Parkinson's disease [1], and/or invading pathogens, for example, antimicrobial peptides (AMPs), a class of amphiphilic and mostly cationic peptides that amongst other target negatively charged bacterial membranes [2]. Studies of peptide–lipid interactions with high structural resolution is thus important to reveal the mechanism behind several human diseases as well as the mode of action of a range of peptides [3].

Small-angle X-ray/neutron scattering (SAXS/SANS) techniques provide *in situ* nanostructural resolution in solution and are therefore well-suited to study peptide–lipid interactions. In particular, SAXS/SANS are useful to resolve both the overall morphological changes (e.g., shape and size from the scattering at low angles that correspond to length scales of a few hundred nm) as well as resolving the more local membrane structure, including the detailed density profiles across the lipid bilayer and chain conformations at larger scattering angles, corresponding to length scales of a few Å [4–7]. With the emergence of more powerful neutron and synchrotron sources, these techniques can also be used to study systems at low (physiologically relevant) concentrations and with temporal resolution starting from a few milliseconds using time-resolved SAXS/SANS [4,5,7]. Neutron scattering is particularly useful because of the sensitivity of neutrons to isotopes, in particular hydrogen (H) and deuterium (D). This can be exploited for contrast variation, which allows structural features (parts of peptide, lipid etc.) or specific kinetic processes to be selectively studied.

A challenge in using small-angle scattering (SAS) to study lipid–peptide interaction in real cells is that the measured signal usually consists of a convoluted average of all components and features in the cell. This makes it hard to resolve the detailed structure of the highly intricate membrane of real cells that consist of a

complex mixture of molecules that are structured in an hierarchical manner. Taking bacteria as an example this already includes a diverse group of membrane proteins, nucleic acids, lipopolysaccharides (LPS) (specifically important constituents of the outer membrane of Gram-negative (G(−)) bacteria), and a vast number of different lipids, where phospholipids are the most abundant. Nevertheless, several groups have explored the possibility of determining structural information of, for example, live bacterial cells from SAS data. Semeraro *et al.* determined the ultrastructure of live *Escherichia coli* bacteria using ultra-SAXS and detailed modelling [8], while Nickels and coworkers have used SANS and contrast variation to characterise the membrane heterogeneities of live *Bacillus subtilis* [9]. Although these studies show that a great deal can be learnt, it is challenging to pinpoint the effects on a detailed molecular level due to the complexity. Thus, there is a need for simplified model systems, where the specific effects of an added compound can be differentiated.

Model lipid membranes, that is, reconstituted, simplistic bilayer membranes that only consist of a few controllable ingredients, allow for a more facile analysis of the interactions. Although the composition is simpler, the key ingredients including the lipids components can be chosen according to the relevancy of the problem at hand. A recent critical review of the relevancy and limitations of model membrane can be found in Ref. [10]. Planar model lipid membranes should be prepared for surface sensitive methods by using supported or free floating bilayers [11]. However, the presence of the interface may alter the membrane properties, for example, spontaneous fluctuations and rigidity, and/or interfere with the interactions, for example, by adsorption of the peptide to the substrate etc. [7] Alternatively, the model membranes can be obtained by making vesicles with rather well-defined and tuneable size. Using well-established protocols, lipid vesicles can be prepared into various structures and are generally divided into unilamellar vesicles (ULVs) consisting of a spherical single bilayer, and multilamellar vesicles (MLVs) that are stacks of spherical bilayers.

For the purpose of small-angle scattering, ULVs are particularly suitable as model system because of the rather well-defined structure and the free accessibility for the peptides to the bilayer membrane. ULVs can also be made asymmetric with differential composition on each leaflet, which thus more closely resembles real cytoplasmic membranes [12,13]. By varying the lipid composition, or using lipid extracts from real cells, substantial insight into complex processes involving membrane interactions can be mapped in more detail.

In this work, we review the latest development and progress in the studies of peptide−lipid interactions using small-angle scattering techniques, particularly focussing on well-controlled vesicular model systems. We will provide an overview of recent work where SAS has been used in combination with model membranes to reveal insight into molecular interactions focussing on the structural and dynamic aspects of peptide−lipid membrane systems. We will briefly review the most relevant theoretical framework before discussing relevant experimental advances highlighting the strengths and possible pitfalls of these techniques.

Small-angle scattering from lipid vesicles with inserted peptides

Following their increased use as models for biological membranes, many different approaches have been put forward in the last few decades on how to describe SAXS and SANS data from ULVs. Broadly, these models can be categorised into either spherical shell models, where one or several shells are used to describe the vesicles [14−18], or radial density profile models where the radial distribution of the various components of the bilayers is taken into account [19−23]. The present work will consider both of these approaches, and in particular focus on how the insertion of peptides into the bilayer of ULVs can be incorporated into the models. In all cases it is crucial, in particular for SAXS analysis, that the change in contrast (e.g., electron density) caused by the peptides is included. Without this modification changes in the scattering pattern caused by simple contrast changes may be falsely interpreted as severe structural alterations of the membrane itself [24]. Furthermore, while increasing the complexity of the analytical models can allow for more detailed descriptions of the bilayer, peptide insertion and the overall structural characteristics of the vesicle, the increased number of parameters introduced can easily lead to overparameterisation if care is not taken. Although a comprehensive treatment of this nuanced topic is outside the scope of the present review, some important considerations are highlighted. Crucially, most of the introduced parameters should not be freely varied, but restricted by using the intensity on an absolute scale and impose molecular constraints. This can be achieved through complementary measurements, and use of literature values (e.g., lipid and peptide volumes), to calculate e.g, scattering length densities, compositions and concentrations. The remaining free parameters (e.g., vesicle size, bilayer thickness and peptide position in the bilayer) should in the fitting procedure be restricted to physically meaningful ranges. The model credibility further increases if it can describe the data over a significant Q range, pertaining to both the overall vesicle shape, size and contrast at low Q and the finer bilayer structure at intermediate to high Q. Similarly, simultaneously fitting multiple experimental data sets (e.g. joint SAXS and SANS analysis [22,24]), while varying only the relevant parameters further reduces the risk of

overfitting. In addition, statistical evaluation of the model through the reduced χ^2 or correlation maps is likely prudent [25,26].

The concentric shells model

In the simplest case, the vesicle can be modelled as a single spherical shell [15]. This, however, does not take into account the different contrast to lipid tail and head groups, which in particular for SAXS analysis is very significant with tails having negative and heads having positive contrast towards water. A more reasonable description can be achieved by using multiple concentric shells to describe the different quasimolecular lipid fragments in the bilayer. With the "three-shell" model [14,17,18], three different shells are used to describe the inner head group, the central tail region and the outer head group, respectively (Figure 1b). Additional shells can be introduced for a finer subdivision of the bilayer, for example by using separate shells for the inner and outer tail groups as in the "four-shell" model [16], or more for even finer bilayer parsing [14,19]. However, the number of shells should be increased with care, due to the risk of overparametrisation.

For a polydisperse concentric shells model, the macroscopic differential scattering cross section can be written as:

$$\frac{d\Sigma}{d\Omega}(Q) = \frac{\phi}{V_{dry}} \int_0^\infty G(R_i) \cdot A_{CS}(Q, R_i)^2 dR_i, \qquad (1)$$

Figure 1

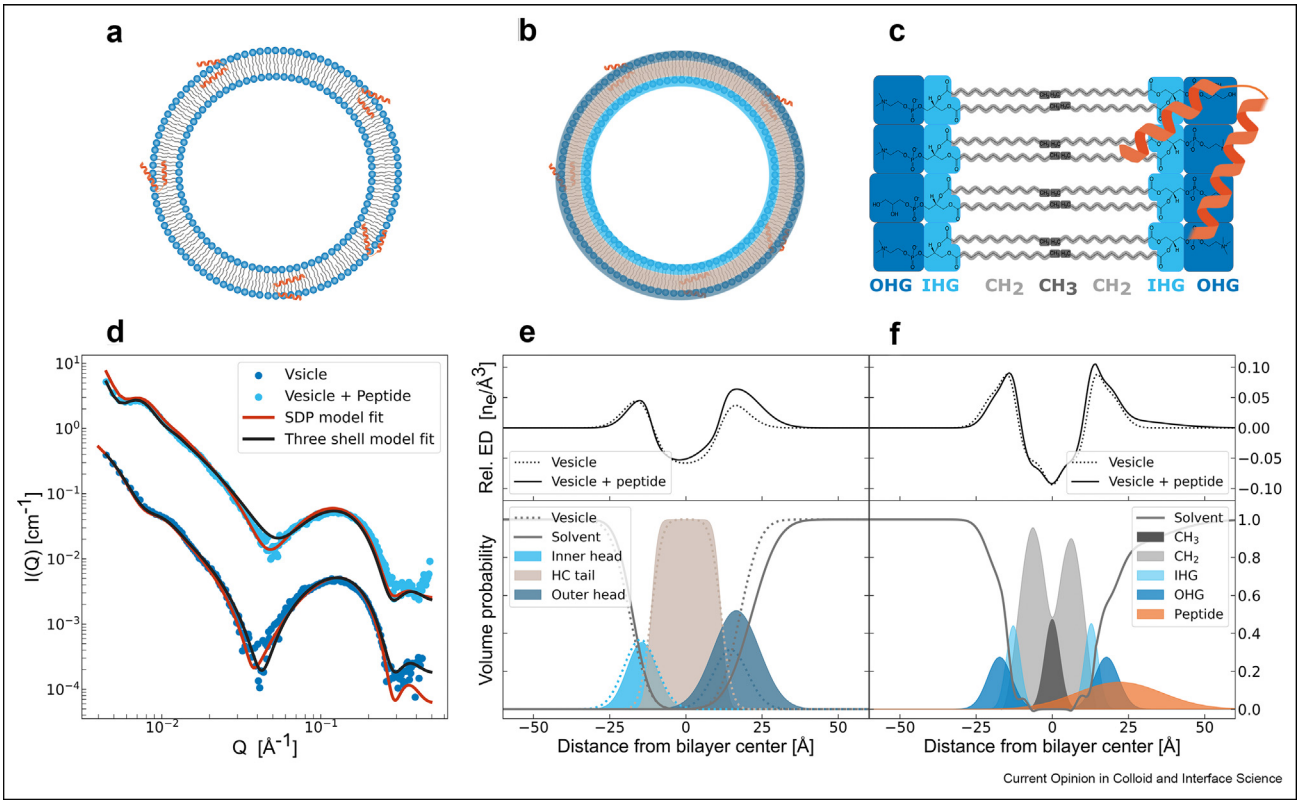

a. Illustration of a vesicle with peptides (Cecropin A used as example) inserted in the interfacial region between head and tails in the outer leaflet of the membrane. **b**. Illustration of the "three-shell" model showing the definition of the three concentric shells in relation to the bilayer structure. **c**. Illustration of the bilayer parsing into outer head group (OHG), inner head group (IHG), methylene (CH_2) and methyl (CH_3) quasimolecular fractions commonly used in the SDP model. Here a mix of 1,2-dimyristoyl-sn-glycero-3-phosphocholine (DMPC) and 1,2-dimyristoyl-sn-glycero-3-phospho-(1′-rac-glycerol) (DMPG) lipids are used as an example. As the two lipids differ in the region comprising the outher head group, an average weighted by the molar fraction of the two lipids is used to determine the volume and number of electrons of the OHG in the SDP model. **d**. SAXS curves from ULVs in aqueous solvent comprised of DMPC (80 mol%) and DMPG (20 mol%), with and without inserted peptide (Cecropin A in a 1:10 peptide:lipid molar ratio). The intensity of the vesicle + peptide curve is scaled by factor 10 for visibility. Experimental data (scattered points) is analysed using both the SDP model (red lines) and the "-three-shell" model (grey lines). **e**. Electron density (ED) profiles with and without peptide (top) and shell volume profiles (bottom) resulting from fitting the "three-shell" model to the experimental data in D. Dotted lines correspond to vesicle only, while filled curves correspond to vesicle with peptide, of which 13% is in the HC shell and 87% in outer head shell. **f**. Electron density (ED) profiles with and without peptide (top) and volume profiles of the quasimolecular lipid fragments (bottom) resulting from fitting the experimental data in D with the SDP model.

where, ϕ is the volume fraction and V_{dry} is the "dry" volume of a single vesicle, corresponding to the combined total volume of the lipids and/or peptides per vesicle without the solvent. $G(R_i)$ is the polydispersity distribution (for example Gaussian) as function of the inner radius of the vesicle, R_i, and $A_{CS}(Q, R_i)$ is the "concentric-shell" amplitude defined as:

$$A_{CS}(Q,R_i) = \sum_{j=1}^{N_S=3,4} \Delta\rho_j \cdot V_j \cdot A_{shell}(Q,R_j,R_{j-1}), \qquad (2)$$

where N_S is the number of shells in the model and $A_{shell}(Q)$ is the scattering amplitude of a spherical shell:

$$A_{shell}(Q) = \frac{1}{V_j}\left[V_s(R_j)\cdot A_s(Q,R_j)\cdot DW(Q,\sigma_j) - V_s(R_{j-1})\cdot A_s(Q,R_{j-1})\cdot DW(Q,\sigma_{j-1})\right], \qquad (3)$$

with $A_s(Q)$ defined as the well-known solid sphere amplitude:

$$A_s(Q,R_j) = \frac{3\sin(QR_j)\cdot QR_j\cos(QR_j)}{(QR_j)^3}. \qquad (4)$$

In the above expressions, V_j is the volume of shell j, while R_j and R_{j-1} are the outer and inner shell radii respectively, and are defined in terms of the inner vesicle radius R_i and the thickness t of each concentric shell up to j. $V_s(R_j)$ is the volume of a sphere of radius R_j. The Debye–Waller factor, $DW(Q,\sigma_j) = \exp(-Q^2\sigma_j^2/2)$, accounts for a diffuse border between the shells [27], and stems from convoluting the sharp radial shell density with a Gaussian, to obtain the smooth profiles shown in Figure 1e. It is worth mentioning that both size polydispersity (eq. (1)) and thermal fluctuations result in a smearing of the scattering curve features. However the effects are mostly affecting different Q regimes, while thermal fluctuations mostly affects the high to intermediate Q, at low Q, polydispersity effects predominates [28].

The amplitude of each shell is scaled by the difference (ie. contrast) between the shell and water scattering length densities (SLDs), ρ_j and ρ^S respectively, as $\Delta\rho_j = \rho_j - \rho^S$. The shell SLD is dependent on the lipid fragment, the amount of inserted peptide, and the degree of hydration of the shell. Defining the number of lipids per vesicle (ie. the lipid aggregation number) as P_{lip}, and the stoichiometric ratio of peptide to lipids as $r_{PL} = n_P/n_L$, the number of peptides per vesicle is given by $P_{pep} = P_{lip} \cdot r_{PL} \cdot \chi^P$, where $\chi_p = 1 - f_{Pfree}$ and f_{Pfree} are the fractions of bound and free peptide in solution respectively. Furthermore, the number of peptides in shell j is given by $P_{pep}\cdot f_j^P$, where f_j^P is the fraction, out of total bound peptide, that is in shell j. Thus there can be a different amount of peptide in each shell, however, $\sum_j f_j^P = 1$ needs to be introduced as a necessary constraint.

Assuming no solvent penetration and no voids, the central hydrocarbon shell should be completely filled with lipid tails and potentially peptides. Under this assumption P_{lip} can be determined from the shell volume, (given by the outer shell radius, R_j, and shell thickness, t_j) and the combined volume of a lipid tail and associated peptide as:

$$P_{lip} = \frac{4\pi[(R_j)^3 - (R_j - t_j)^3]}{3(V_{tail} + r_{PL}\chi^P f_{HC}^P V_P)}, \qquad (5)$$

where V_P and V_{tail} are the peptide and lipid tail volumes, respectively. However, as there is less volume in the inner bilayer leaflet it will contain fewer lipids compared to the outer leaflet. If the tail region is described by a single shell, as in the "threeshell" model, the number of lipids in each leaflet can be expressed as $P_{lip}\cdot\chi_{leaf}^L$, with $\chi_{outer}^L = (R_j^3 - (R_j - t_j/2)^3)/(R_j^3 - (R_j - t_j)^3)$ for the outer leaflet and $\chi_{inner}^L = 1 - \chi_{outer}^L$ for the inner, with $j = 2$ in this case.

Using P_{lip}, the volume fraction of the lipid fragment (head or tail), ϕ_j^L, peptide ϕ_j^P and solvent ϕ_j^S in each shell can be determined as:

$$\begin{aligned}\phi_j^L &= \left(P_{lip}\cdot\chi_{leaf}^L\cdot V_j^L\right)/V_j \\ \phi_j^P &= \left(P_{lip}\cdot\chi_{leaf}^L\cdot r_{PL}\cdot\chi^P\cdot f_j^P\cdot V_P\right)/V_j \\ \phi_j^S &= 1 - \phi_j^{lip} - \phi_j^P\end{aligned} \qquad (6)$$

where V_j^L is the volume of the lipid fragment. It is emphasised that for the single hydrocarbon shell ($j = 2$) in the "three-shell" model, $\chi_{leaf}^L = 1$, and $\phi_2^S = 0$, as $\phi_2^L + \phi_2^P = 1$ per definition. If different shells are used for the inner and outer tail groups (ie. the "four-shell" model), equation (5) can be used to compute separate lipid aggregation numbers. The SLD of each shell is then calculated as:

$$\rho_j = \phi_j^L\rho_L^j + \phi_j^P\rho_P + \phi_j^S\rho_S, \qquad (7)$$

where ρ_L^j, ρ_P and ρ_S are the "dry" SLDs of the lipid fragment, the peptide and the solvent, respectively. Finally, $V_{dry} = P_{lip}V_{lip} + P_{pep}V_P$ which is used in equation (1) to determine the number of scatterers. The free fitting parameters are therefore the geometrical parameters of the shells (inner radius and polydispersity, thickness of each shell and the smearing parameter σ in the DW factor) as well as the fractions of peptide in each shell, together with the fraction of free peptide. The remaining parameters are either independently determined, or directly derived from the aforementioned parameters. It bears mentioning that

as the insertion of peptide in the inner and outer head group shells can displace the solvent, a restriction should be introduced to prevent negative solvent fractions.

Experimental SAXS data of vesicles comprised of 1,2-dimyristoyl-sn-glycero-3-phosphocholine (DMPC) and 1,2-dimyristoyl-sn-glycero-3-phospho-(1′-rac-glycerol) (DMPG) in a 80:20 M ratio, with and without inserted peptide (Cecropin A in a 1:10 peptide:lipid molar ratio), analysed with the "three-shell" model are shown in Figure 1d with the resulting shell volume probabilities and electron density profiles shown in Figure 1e. In this case the model fits reasonably well, especially for the scattering from pure vesicles, but does not fully explain the scattering with added peptide, particularly the minimum at intermediate Q. With only three shells the model presents a coarse-grained description of the bilayer structure with limited asymmetry as both tails are described by a single shell, and limited resolution of the peptide insertion, which might be particularly challenging in the case of Cecropin A which is shown to have a very broad and asymmetric distribution in the bilayer [29]. Higher resolution of the bilayer structure can potentially be achieved by increasing the number of shells, like in the case of the "four-shell" model used by Qian *et al.* to describe SANS data of vesicles with peptide induced asymmetry [16]. Care has to be taken however, as increasing the number of shells rapidly increases the number of free parameters, especially if the peptide distribution is allowed to vary between the shells.

The scattering density profile (SDP) model

In order to provide a more realistic description of the peptide insertion, the radial density profile of the peptide and lipid components in the bilayer can be described by a continuous function rather than discrete shells. Although explicit radial density profiles can be introduced and the total scattered intensity computed via a 3D Fourier transform [15], the description is significantly simplified by assuming that the bilayer is locally flat. This is a valid approximation when curvature is low, that is, when the inner vesicle radius, R_i is sufficiently large compared to the bilayer thickness t, with $t/R_i < 0.5$ [15]. Under these circumstances the radial and lateral scattering contributions can be treated independently using the separated form factor (SFF) approximation: [15,30].

$$I(Q) \simeq S(Q) \cdot |F_{TS}\ (Q)|^2 \cdot |F_{FB}\ (Q)|^2 \tag{8}$$

where $S(Q)$ is the structure factor, $F_{TS} = 4\pi R^2 \frac{\sin(QR)}{QR}$ is the form factor of an infinitely thin spherical shell with radius R, and F_{FB} is the form factor of a flat bilayer sheet which contains information about the distribution of the lipid components across the bilayer. Brzustowicz and Brunger showed that the scattering from asymmetric vesicles can be described using a smooth SLD model function [20]. In this case the SLD is described by a sum of three Gaussian functions, one each for the head groups and one for the tail groups. It is important to point out that for small vesicles, curvature effects may lead to asymmetric SLD profiles even for vesicles with uniform lipid compositions at both leaflets [28]. The flat bilayer formfactor can then be described as:

$$|F_{FB}| = \left| \int_{-D_i}^{D_o} \Delta\rho \exp(iQz) dz \right| = \sqrt{(F_{cos}^2 + F_{sin}^2)}, \tag{9}$$

where $F_{cos} = \int_{-D_i}^{D_o} \Delta\rho \cos(Qz) dz$ and $F_{sin} = \int_{-D_i}^{D_o} \Delta\rho \sin(Qz) dz$ are the real and imaginary terms of F_{FB}, with the integrals extending from the innermost distance D_i to the outermost distance D_o in the bilayer.

This is followed by the scattering density profile (SDP) model, presented by Kučerka and coworkers [21,31,32], where the bilayer is described by one-dimensional Gaussian volume probabilities of quasimolecular lipid fragments (with a typical parsing shown in Figure 1c):

$$P_i(z) = \frac{c_i}{(2\pi)^{1/2}} \exp\left[-\frac{(z - z_i)^2}{2\sigma_i^2} \right], \tag{10}$$

where i represents the specific quasimolecular lipid fragment, while z_i is the position and σ_i the width of the distribution, and $c_i = V_i/(A_L\sigma_i)$, with V_i and A_L defined as the volume of the lipid fragment and area per lipid, respectively. It is important to stress that for the SLD or electron density to be determined quantitatively, the specific volumes of each component (lipid and peptide) must be determined separately, through, for example, volumetric measurements and/or the use of literature data [33,34]. Alternatively, only the relative profiles can be determined [35]. To account for the potential asymmetry in the inner and outer hydrocarbon tail regions and to enforce that no water is present in the bilayer core, the hydrocarbon region can be described by a half-period squared sine/cosine function rather than by additional Gaussians, as described by Eicher *et al.*: [22].

$$P_{HC}(z) = \begin{cases} \sin^2\left(\frac{\pi}{2} \cdot \frac{z - z_{MN_i} + \sigma_{HC_i}}{2\sigma_{HC_i}}\right), \\ \quad \text{for } z_{HC_i} - \sigma_{HC_i} \le z < z_{HC_i} + \sigma_{HC_i} \\ 1, \\ \quad \text{for } z_{HC_i} + \sigma_{HC_i} \le z < z_{HC_o} - \sigma_{HC_o} \\ \cos^2\left(\frac{\pi}{2} \cdot \frac{z - z_{HC_o} + \sigma_{HC_o}}{2\sigma_{HCo}}\right), \\ \quad \text{for } z_{HC_o} - \sigma_{HC_o} \le z < z_{HC_o} + \sigma_{HC_o} \end{cases} \tag{11}$$

where $z_{HC_{i,o}}$ is the 0.5-probability value for the HC group and $2\sigma_{HC_{i,o}}$ is the width of the squared sine/cosine

functions. The probability function for the CH_2 groups is then determined as $P_{CH_2}(z) = P_{HC}(z) - P_{HC_3}(z)$. Finally, space filling is ensured by calculating the solvent probability last as $P_s(z) = 1 - \sum_i P_i(z)$ [32]. The volume probability profiles (Figure 1f) are then scaled by the SLDs of the corresponding fragments, using either the number of electrons (for SAXS) or the total coherent neutrons scattering length (for SANS), also allowing for joint analysis.

The insertion of peptide can be described by adding the peptide as an additional Gaussian (eq. (10)) scaled by the peptide volume, V_p, total volume fraction, f_p of added peptide and by the fraction of peptide associated with the bilayer χ^P, with $c_p = (V_p f_p \chi^P)/(A_L \sigma_p)$ as shown by Nielsen *et al.* [24]. The peptide partitioning in the bilayer can with this be varied continuously, allowing for a more detailed description of its insertion and position in the bilayer [24,29]. However, the change in SLD is dependent on the fraction of peptide in the tail and head regions respectively, which has to be taken into account. The contrast contribution from the peptide can be described as:

$$\Delta\rho_P(z) = f_{p,tail} \cdot (\rho_P - \rho_{HC}) + (1 - f_{p,tail}) \cdot (\rho_P - \rho_S), \tag{12}$$

where ρ_P, ρ_{HC} and ρ_S are the peptide, hydrocarbon tail, and solvent SLDs respectively, while $f_{p,tail}$ is the fraction of peptide in the tail region and is defined as the integral of the overlap with the hydrocarbon volume probability:

$$f_{p,tail} = \frac{\int_{z_p - 5\sigma_p}^{z_{int}} P_{HC}\, dz + \int_{z_{int}}^{z_{HC}+\sigma_{CH2}} P_P\, dz}{\int_{-\infty}^{\infty} P_P\, dz}, \tag{13}$$

where P_{HC} and P_P are the volume probability functions, with the corresponding positions z_{HC}, z_P and uncertainties σ_{HC}, σ_P of the hydrocarbon region and peptide respectively. z_{int} is the intersect between the two overlapping probabilities and can be determined numerically, for example, using the well-known Brent-Dekker method. For the analytical solution for the flat bilayer form factor in equation (9) with inserted peptide it is referred to Ref. [24]. Experimental SAXS data for vesicles with and without peptide are analysed with the SDP model (Figure 1d) with the resulting volume and electron density profiles shown in Figure 1f.

A complication arises when the peptide not only inserts, but also solubilises the membrane. This is prone to happen at high peptide:lipid (P:L) ratios for, for example, AMPs [36,37] or α-synucleins [38], and demands the introduction of coexistence models that also include micellar aggregates. This can often be detected as a decrease in the overall intensity of the broad peak of the bilayer scattering and additional contributions at intermediate Q [18]. Since this introduces a significant amount of free parameters, care must be taken in the analysis to avoid ambiguities, it is therefore in most cases preferable to work at lower P:L ratios.

Probing the nanostructure: peptide and lipid membrane interactions

Antimicrobial peptides

There are many relevant questions that relates to how AMPs interact with cell membranes that can be addressed by SAS techniques. Examples includes how AMPs affect the membrane structure (thickening/thinning), peptide insertion and position in the membrane and thus whether AMPs can create pores in the cytoplasmic membrane. Other relevant questions relates to whether the AMPs disturb the packing, solubilise the lipid membrane or cross the membrane for intracellular targets [2].

Recently Semeraro *et al.* reported the real-time response of *E. coli* to lactoferricin-derived AMPs using TR-SAXS experiments [39]. SAXS together with electron microscopy (EM) data revealed how the AMPs rapidly permeabilise the cytosolic membrane within less than 3 s, and damage of the cell envelope occurred even at sublethal peptide concentrations, implying that the impairment of the membrane barrier is a necessary but not sufficient condition for microbial killing by lactoferricins. This study shows the information that can be gained by careful analysis of SAS data even in "live" cells.

Despite this recent breakthrough in the ability to study membrane interactions even in live bacterial cells using SAS, most of the available studies are done using model membranes such as lipid vesicle systems. This has the benefit that also more subtle membrane effects of AMPs can be resolved. In many of these studies bacterial membranes are crudely mimicked by mixtures of anionic and zwitterionic lipid mixtures, which roughly corresponds to the net charge of a typical bacterial cell membrane. However, positively charged peptides, such as AMPs, will often cause vesicles to aggregate and/or fuse leading to unstable colloidal suspensions that may form a variety of structures such as MLVs or large nonlamellar phases, which may also precipitate out of solution [40]. While such phenomena may be relevant as an important mechanism to how bacteria are disrupted, the information on insertion and structuring of AMPs within the bilayer will be obscured. One method to prevent this is to add a small amount of PEGylated lipids, which provide entropic repulsion between the vesicles [24,29,41]. In this way, the (unilamellar) membrane is accessible for the peptide while at the same time the bilayer structure remains intact allowing for more accurate quantitative analysis.

The α-helical AMP LL-37 is the only human cathelicidin, and is therefore one of the most well studied

AMPs. LL-37 has pleiotropic properties, as a key player in the human innate immune system with broad spectrum antimicrobial activity, immunomodulation abilities etc. Sevcsik *et al.* first showed how LL-37 can solubilise 1,2-dipalmitoyl-sn-glycero-3-phosphocholine (DPPC) lipid vesicles resulting in a co-existence of two populations of membrane structures (discs and extended bilayers) [36,37]. Freire *et al.* suggested that, depending on the peptide:lipid (P:L) ratio, cylindrical mixed micelles were formed in 1-palmitoyl-2-oleoyl-sn-glycero-3-phosphocholin (POPC)/1-palmitoyl-2-oleoyl-sn-glycero-3-phospho-(1′-rac-glycerol) (POPG) lipid vesicles [42]. Nielsen *et al.* further showed that these effects are both dependent on the P:L ratio as to be expected [29], but also to the composition of the lipid bilayer, where bilayers composed of PE/PG-lipids are solubilised at a lower LL-37 concentration than bilayers with PC/PG-lipids [41]. Similarly, Freire *et al.* observed a structural transformations from vesicles to mixed cylindrically shaped micelles upon addition of LL-37 in increasing amounts to pure PG vesicles, as observed by SAXS together with dynamic light scattering (DLS), transmission electron microscopy (TEM) and molecular dynamics (MD) simulations [42]. These SAS results seen together support a potential detergent like mode of action of LL-37 when present in high concentrations. However, at lower L:P ratios the peptide inserts into the membrane without causing solubilisation, pointing towards less invasive membrane effects, for example the interface activity model where peptide induced changes in the lipid packing is related to membrane leakage [43], pore formation, changes in lipid dynamics [29], in addition to known intracellular effects of LL-37 [44].

Indolicidin, is another cathelicidin peptide, originating from bovine neutrophils. Contrary to most AMPs, it is mainly unstructured monomeric in aqueous solution, as confirmed by SAXS [24]. Using different model membranes and by developing an advanced theoretical model, based on the existing SDP model, to describe the scattering from different contributions of the lipid/peptide components Nielsen *et al.* demonstrated that indolicidin is preferentially located at the interface between the tail and head groups on the outer leaflet, consistent with the interface activity model described above, at a range of physiologically relevant concentrations without causing solubilisation of the membrane as observed for LL-37 [24]. This approach of detailed model analysis of the peptide position in a lipid membrane was verified to be accurate by comparing the results directly to data from neutron reflectometry (NR) using the same lipid composition, indolicidin batch and lipid to peptide ratios [45].

Defensins are another potent class of AMPs found in humans. By using SAXS Schmidt *et al.* investigated the interactions between liposomes mimicking either bacterial membranes or eukaryote membranes, and various members of the defensin subfamilies, α-defensins, β-defensins, and θ-defensins [46]. The results revealed that these AMPs selectively permeabilise the bacterial model membranes, and generate negative Gaussian membrane curvature, referred to as saddle-splay. This is a necessary condition for processes such as pore formation, blebbing, budding, and vesicularisation, and SAXS data in this way gives new insight into the mode of action of this group om AMPs.

Peptides isolated from frogs form a substantial class of AMPs, which have been extensively studied for their membrane effects by SAS. One example is peptidyl-glycylleucine-carboxyamide (PGLa), from South African clawed frogs, which was found by Pabst *et al.* using SAXS and WAXS to change the structure and fluidity of lipid membranes at different temperatures [47]. From the analysis using the SDP model they were able to determine a 1−2 Å increase in the thickness of 1,2-dimyristoyl-sn-glycero-3-phospho-(1′-rac-glycerol) (DMPG) and 1,2-dipalmitoyl-sn-glycero-3-phospho-(1′-rac-glycerol) (DPPG) vesicles as induced by the peptide, when the lipids where in the fluid phase [47]. They later compared the membrane effect of L18W-PGLa to that of magainin II, another AMP sourced from frogs. In this study they did SANS, SAXS, nuclear magnetic resonance (NMR) and molecular dynamics (MD) simulations to obtain a detailed picture of how the two AMPs either alone or in synergy insert into lipid membranes. In this case they observed membrane thinning for both AMPs as a result of a change in the lipid packing, as well as a stronger penetrative effect upon dimerisation of the peptides as confirmed by MD simulations, fitting better with the experimental SAS data, illustrating the power of combining SAS and MD simulations [48]. Further they showed that these peptides cause vesicle adhesion and fusion within a few seconds [40], resulting in a growth of the vesicles that similarly has been observed, in a concentration dependent matter, for other AMPs like indolicidin [49].

Nielsen *et al.* used SAXS to compare the membrane effect of a range of natural AMPs directly using the same instrument, analysis, lipid vesicle system and lipid:-peptide ratio. The AMPs include magainin II, aurein 2.2, lacticin Q, cecropin A, colistin and LL-37 (results previously discussed above). By using a similar approach as for indolicidin as described above, detailed analysis of the SAXS data revealed that the membrane effects and insertion of these peptides varied significantly. While for example magainin II, cecropin A and lacticin Q inserted in the outer leaflet of the membrane, aurein 2.2 rather inserted transmembrane [29,41]. The transmembrane positioning can correlate with a traditional pore formation mechanism of bacterial killing, however the other AMPs that are found to position in the outer leaflet do

not. In these cases a different mechanism of disturbed lipid packing (as supported by changes in the lipid phase transition temperature) that could result in fluid or ion leakage [43] or changes in lipid dynamics as discussed in the next chapter seems more likely.

The peptide melittin, is derived from a honey bee (*Apis mellifera*) venom, and is often referred to as an AMP although it lacks selectivity towards microbial cells. Using aligned multistacked lipid membranes where the peptide is prepared with brominated lipids, White and coworkers showed that melittin causes minimal perturbation of the lipid membrane at low concentrations, but larger effects on the membrane are observed when a high concentration of peptide is added [50]. Using the same method, Lee *et al.* also suggest that stable pores only are formed above a critical peptide-to-lipid ratio [51]. Using ULVs and SANS, Heller and coworkers suggested that the membrane thickness can be both thicker or thinner in response to peptide exposure depending on concentration and lipid composition [17].

Colistin (polymyxin E) is an AMP produced by the soil bacterium *Bacillus polymyxa*. It is currently used in clinics as a last-resort treatment for multidrug-resistant Gram-negative (G(−)) infections, and has therefore been extensively studied by a range of different techniques including SAS. SAXS on hydrated multi-stacks of lipid bilayers was used by Dupuy *et al.* to determine the interactions of colistin (polymyxin E) with model membranes containing 1-palmitoyl-2-oleoyl-sn-glycero-3-phosphoethanolamine (POPE)/POPG/cardiolipin and POPG/1,2-dioleoyl-3-trimethylammonium-propane(-DOTAP)/POPE/cardiolipin to mimic the cytoplasmic membrane of G(−) bacteria and gram-positive (G(+)) bacteria, respectively [52]. They found that the peptide inserts in the interfacial area between head and tail in both cases, and partitions more deeply into the inner membrane of G(−), locating right under the headgroup, while remains in the headgroup region in the G(+) mimicking membrane [52]. While Nielsen *et al.* found using ULVs rather than multi-lamellar stacks, but with a simpler lipid composition of only DMPC/DMPG and 1,2-dimyristoyl-sn-glycero-3-phosphoethanolamine (DMPE)/DMPG that colistin did not interact with the liposomes over a range of concentrations [29,41].

Natural AMPs is not the only class that has been studied using SAS, also *de novo* designed AMPs and peptide-mimics have been subject of investigation using SAS. Hamley, Castelletto and coworkers have done extensive work in this field using a combination of TEM and SAXS. For example, they found that the lipid vesicle interaction of surfactant-like arginine-rich peptides highly depends on the number of arginine residues in the peptide structure. They also describe peptide induced formation of multilamellar vesicles [53,54]. Further they found using SAXS, that peptides that contain blocks of symmetric charged (arginine) and hydrophobic (phenylalanine) residues interact with lipid bilayers by inducing correlation between bilayers (R3F3), or by causing an increase in polydispersity of the vesicle wall thickness (R4F4) [55].

All-D-AMP peptides have been studied for their increased *in vivo* enzymatic stability over the natural occurring L-AMP counterparts. Lone *et al.* determined by SAXS how their library of all-D-peptides had a lower membrane bound amount when comparing with previously studied L-peptides. In addition to the membrane effects, SAXS was also used in this paper to compare the propensity of the peptides to self-assemble into defined nanoparticles of hollow tubes, and sheets, which could be relevant for their *in vivo* activity, showing the diversity of the technique in the study of peptides [56]. While Heinrich *et al.* used SAXS on oriented stacks of lipid membranes in combination with NR to compare the membrane effect of two peptides WLBU2 and D8 (all 8 valines are the D-enantiomer), revealing that both peptides cause membrane thinning and dual location in the membrane headgroup and hydrocarbon region [57].

Cyclisation of peptides is another strategy for improvement of enzymatic stability of AMPs. Recently, Lone *et al.* described how the cyclic version of incolicidin inserts into the bilayer of lipid vesicles very similarly as the natural linear peptide suggesting a comparable mechanism of action [58].

SAS has further been used to study *de novo* designed self-assembling AMPs, in order to investigate how the presence of lipid membranes may affect the physical stability of the self-assembled structures. One example is the beta-sheet nanofibers based on the general $K_x(QL)_yK_z$ motif, which self-assembles into elongated fibres consisting of two stacked beta sheets, held together by hydrophobic interaction of the leucine residues, as shown by amongst other SAXS [59]. By using SANS and contrast matched liposomes Nielsen *et al.* showed that the fibres are exceptionally stable even in the presence of lipid membranes, indicating that the fibres in themselves have antimicrobial activity [60].

Von Gundlach *et al.* has developed a method using SAXS data on *E. coli* cells treated with different antibiotics including AMPs as a high-throughput method for screening of mode of action of the substances by distinguishing the changes in the SAXS curves of several antibiotics with well-known mode of action by principal component analysis. This enables them to distinguish

AMP drug candidates with novel mode of actions from the established antibiotics for further development in the matter of minutes rather than days or weeks as conventional tests to identify the mode of action used today [61].

Amyloid forming peptides

Amyloid oligiomerisation and fibrilisation has been extensively researched over the past decades because of their link to disease development, and suggested role in the innate immune system. These amyloid forming peptides are also considered surface active, and may perturb both the structure and the integrity of lipid membranes, as well as the presence of lipid membranes has been found to trigger amyloid formation [1].

Using a combination of SANS on peptide−vesicle mixtures, analysed using a three-shell model Rai *et al.* revealed how β-amyloids (Aβ), which are linked to Alzheimer's disease, inserts into charged DMPG bilayers in the interfacial region between water and hydrocarbon chain (Figure 2a), similarly to a series of AMPs, while it doesn't penetrate deeply into the bilayer [17]. While, Dante *et al.* determined using SANS and the SDP model that Aβ_{1-42} causes an increase in the liposome radii which they explained by vesicle fusion. Carrotta *et al.* used SAXS data to study how Aβ interaction with lipid vesicles changes with addition of varying amounts of sphingomyelin, ganglioside and cholesterol to the lipid vesicle composition [65]. Ivankov *et al.* has used SANS to characterise spontaneous reformation of ULVs to discoidal bicelle-like structures and small ULVs with increasing temperature to above the thermodynamic phase transition of the lipids, selectively in the presence of the Aβ_{25-35} peptide as shown in Figure 2b [62].

Figure 2

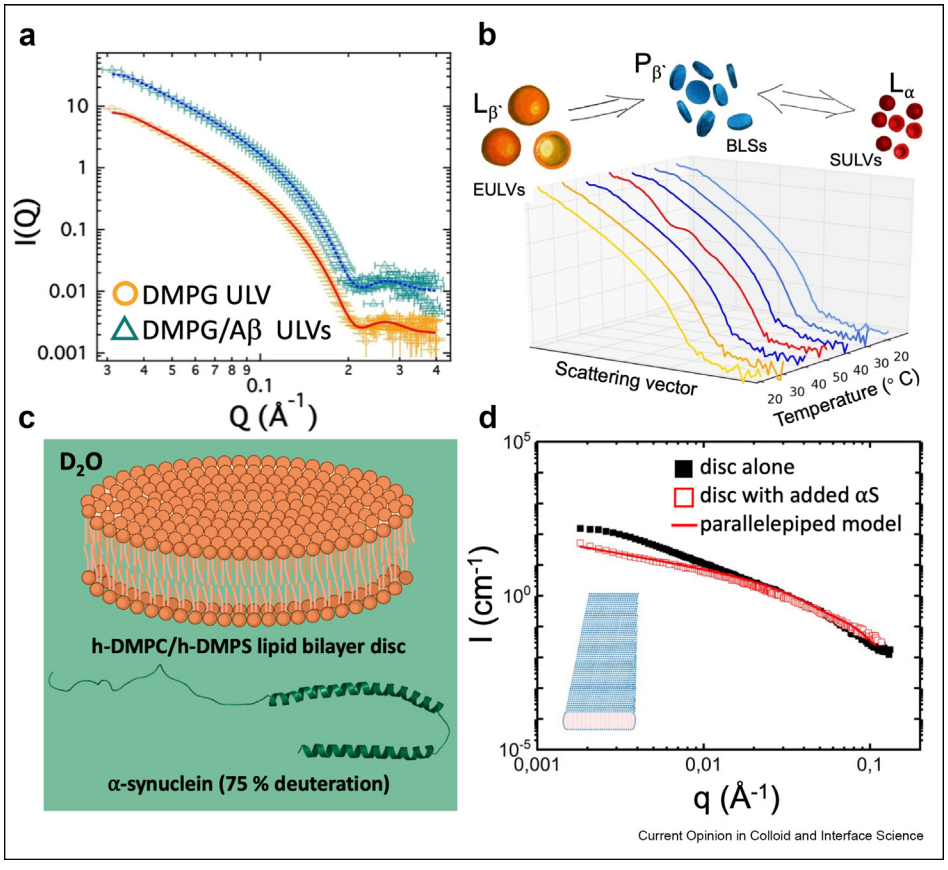

a. SANS data on DMPG liposomes and DMPG liposomes mixed with Aβ peptide in 100%. D_2O with respective fits using the three-shell model. Figure is reproduced from Ref. [17]. **b**. SANS data on DPPC/Aβ_{25-35} membrane organisations as a function of increasing temperature. The best fit model to describe the SANS curves are indicated with corresponding colours in the illustration above. Figure is reproduced from Ref. [62]. **c**. Illustration of the SANS method used to obtain data presented in figure **d**, utilising contrast matching of 75% deuterated αS protein (PDB:1XQ8 [63]) to extract information on peptide induced changes in the lipid bilayer discs. Created with BioRender.com. **d**. Scattering profiles of a pure lipid bilayer disc dispersions in 100%. D_2O, and of the changes induced after addition of αS, and best fit with a parallelepiped (illustration inset) model with a length of shorter edge a = 13 nm and a length of longer edge b = 550 nm. Figure is reproduced from Ref. [64].

Olsson and coworkers recently presented data revealing that the structure of α-synuclein (αS) fibrils, which has been linked to development of Parkinson's disease, composed of two photofibrils is not affected by coaggregation with lipids [66], similar results was found in a study on the central protein fragment NACore [67]. However, using time resolved SANS (TR-SANS) in combination with deuterated αS proteins (Figure 2c), they obtained the needed contrast between the amyloid and lipid membrane and were able to determine that the shape of the lipid nanodiscs is highly depended on the interaction with the amyloid protein and its oligomerisation state (Figure 2d). Previously circular discs transformed into elongated parallelepiped shapes upon absorption of nonfibrillated αS as confirmed by cryo-EM, but upon αS fibrilisation the amyloid molecules desorb from the bilayer and the circular discs regain their original shape [64]. A recent study by Galvagnion *et al.* on αS fibrilisation confirmed that αS cause solubilisation and structural transformation of vesicles. However, they suggest that the lipids take an active role in the process of nucleation of fibrils beyond simply acting as surface catalysts. They find using TR-SAXS and a stopped-flow apparatus (SFA) that the binding of the protein to the vesicles induces a very rapid structural transition (less than 2−3 ms) into lipid−peptide nanoparticles of disc-like and/or cylindrical shape, which after incubation for several hours further transitions into traditional amyloid fibril formation, but where the lipids are incorporated into the fibrils [38].

Using contrast variation and SANS Martel *et al.* found that the aggregates formed by human islet amyloid poly peptide (IAPP), which is a peptide linked to the development of type 2 diabetes, where larger in presence of 1-palmitoyl-2-oleoyl-glycero-3-phosphocholine (POPC) lipids than the aggregates formed in its absence. They estimated based on these data that the aggregates are constituted of 70% peptide and 30% lipids [68], indicating that the peptide and lipids co-aggregate similarly to what Galvagnion *et al.* found for αS [38].

Beyond the natural amyloid peptides, SAS has further been used to explore the amyloid like fibril formation of short model peptides in model membranes. Gerbelli *et al.* determined how two amyloid forming short peptides, [RF] and $[RF]_4$ (where R = arginine and F = phenylalanine) caused changes in the structure of DPPC membranes with increasing peptide concentration, including formation of MLVs and increased thickness of the bilayer [69].

pH responsive peptides

The effect of peptides that selectively interact with lipid membranes upon changes in pH can also be probed by SAS. Narayanan, Reshetnyak, Engelman and coworkers studied the pH Low Insertion Peptides (pHLIP) derived from bacteriorhodopsin, which show a pH dependent coil−helix transition that is accompanied by a change in the insertion mechanism into lipid bilayer membrane using SAXS and unilamellar POPC liposomes [70]. They showed that at low pH, the peptide inserts into the membrane in a transmembrane like fashion, while at higher pH values, the inner hydrophobic part of the electron density profile has a similar shape as in pure POPC liposomes, indicating that the peptide molecules were residing at the outer leaflets of the membranes. The transition, which can be used to target (more acidic) tumour cells, is driven by aspartic acid residues which become neutralised at low pH thereby facilitating alpha-helix formation and transmembrane insertion.

Probing kinetics: from structural transformations to lipid diffusion

Cell membranes are not static entities and exhibit rather rich dynamic behaviour, from larger scale shape fluctuations to local diffusion of individual molecules. For example, it is well-known that lipid vesicles undergo shape fluctuations and membrane undulations that can be conveniently studied by neutron spin-echo (NSE) spectroscopy [71]. Shape fluctuations will also affect the static (average) SAS data in a manner that is challenging separate from polydispersity [28]. In response to changes in temperature, pH, salt etc, or by addition of surface active molecules such as detergents or peptides, vesicles may undergo morphological transitions [36,37,40,72,73]. SAS can be used to probe various kinetic processes [4,5]. In particular, by taking advantage of the high brilliance of the X-ray beams in synchrotrons, allowing structural resolution of processes down to a few milliseconds [4,5,74]. TR-SAXS has been used to investigate nonequilibrium kinetics associated with structural transformation of lipid vesicles exposed to detergents [73], osmotic shocks [75], and AMPs [76]. The latter study showed that nonsterically stabilised liposomes (POPE/POPG/cardiolipin) form MLVs and eventually phase separate on time scales of a few minutes after peptide exposure.

In addition to nonequilibrium structural transitions, TR-SANS allows us to probe the dynamics of lipid membranes at equilibrium. Using a method originally developed for micellar systems [4], both the transversal exchange between leaflets, lipid "flip-flop," and exchange between vesicles can be probed [7,77,78]. The method, illustrated in Figure 3a, is based on hydrogen/deuterium (H/D) contrast variation where deuterated and proteated vesicles are mixed in a solvent that matches the average SLD of the two. Upon mixing on the molecular scale, the intensity will drop rendering the kinetics visible (Figure 3b). Contrary to other methods such as fluorescence and temperature-jump experiments, this method does not require labelling with bulky chemical groups or perturbation from equilibrium.

Figure 3

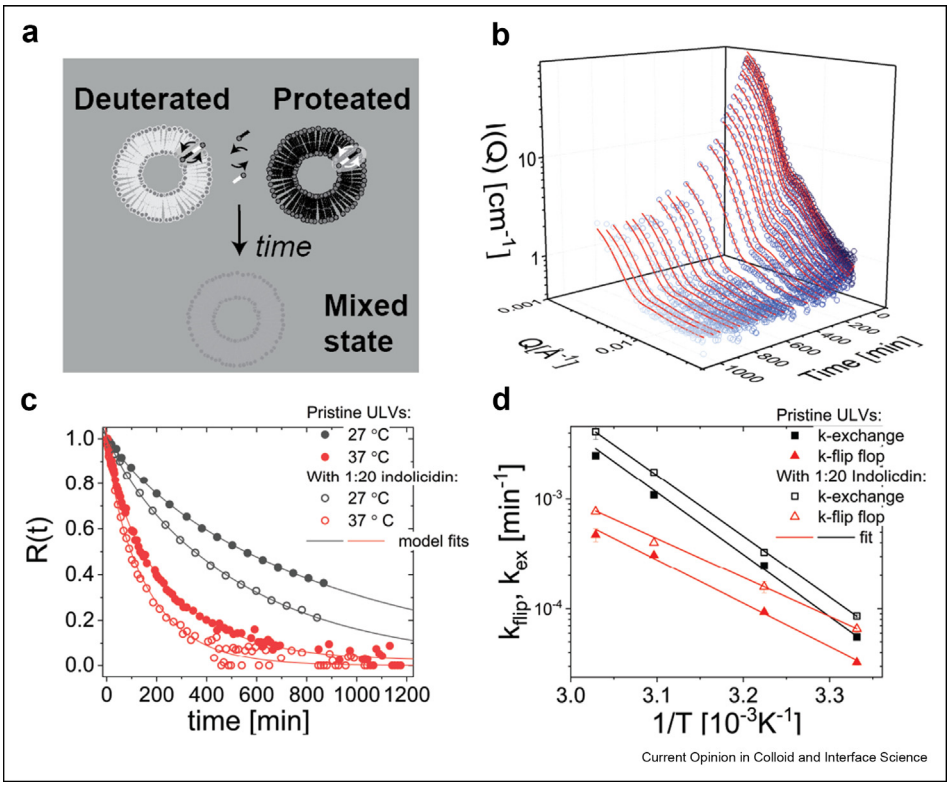

a. Illustration of the TR-SANS utilising the zero-average contrast variation to extract the lipid dynamics. In short, H- and D-vesicles is mixed in a buffer solution that matches the *average* H/D composition. **b**. TR-SANS data showing the decay in time for DMPC/DMPG vesicles with corresponding fits. **c**. The decay in the overall contrast, $R(t)$, for the same vesicles with and without addition of indolicidin. **d**. Corresponding Arrhenius plots. All data reproduced from Ref. [49].

The technique was first successfully applied to extract lipid flip-flop and exchange in unilamellar DMPC vesicles [77]. The results can be quantified by the relaxation function, $R(t) = (I(t) - I_\infty)/(I(t=0) - I_\infty)$, where $I(t)$ is the (integral) time-dependent intensity, while $I(t=0)$ and I_∞ are the intensities at the beginning and after complex (molecular) mixing, respectively (Figure 3c). Alternatively, the complete TR-SANS data can be analysed with time-dependent scattering model [4,49,79,80] from which we can extract the fraction of "labelled" lipids per vesicles, $f(t)$ as a function of time, $0 \leq f(t) \leq 1$. Both can be described by a double exponential function reflecting the two possible diffusion processes:

$$R(t) = \left(\frac{1}{2} - \frac{k_f}{X}\right)\exp\left(-\frac{k_{ex} + 2k_f + X}{2}t\right) + \left(\frac{1}{2} + \frac{k_f}{X}\right)\exp\left(-\frac{k_{ex} + 2k_f - X}{2}t\right) \quad (14)$$

where $X = \sqrt{4k_f^2 + k_{ex}^2}$, k_f and k_{ex} are the rate constants for flip-flop and exchange respectively.

It has been shown that additives such as methanol or simple changes in curvature of ULVs accelerate the lipid kinetics. Nielsen *et al.* investigated the dynamics of DMPC/DMPG lipids in ULVs stabilised by small amounts of h-DMPE-PEG, and exposed the vesicles to a series of natural AMPs with different degree of interaction with the membrane. The data showed that all AMPs except colistin (polymyxin E) significantly enhanced the rate of both flip-flop and exchange kinetics between the vesicles. The effect was similar even though insertion varied from creating a transmembrane-like structure to preferential location in the head/tail group interface [29]. Interestingly by selectively labelling the DMPC, it was deduced that DMPG lipids flip slightly faster than DMPC but are similarly affected by the peptide [49]. The lack of interactions with colistin was also found for DMPE/DMPG/DMPE-PEG vesicles, in contrast to lipid membranes used in other studies [52,81]. Here aurein 2.2, indolicidin, LL-37 and lacticin Q significantly accelerated the lipid kinetics while colistin did not. Through a more detailed Arrhenius analysis of the rate constants it was found, perhaps surprisingly that neither indolicidin nor LL-37 affected

the activation energy for flip-flop, E_a^{flip}, significantly [29]. However, the data showed an increase in the prefactor that can be attributed to an increase in the transition entropy showing that the AMPs disorder the membrane leading to acceleration. For the exchange kinetics, however, it was observed that LL-37 reduces the activation energy, $E_a^{ex.}$, while it remained essentially unaltered in the case of indolicidin. This might indicate that LL-37, which solubilises the membrane at higher P:L ratios [36,37], is able to form complexes with individual lipids leading to more rapid exchange. Nguyen *et al.* investigated the effect of a methanol solution containing the AMP, alamethicin and melittin, on the dynamics of DMPC vesicles using TR-SANS [82]. They found that both peptides accelerated the flip-flop and exchange processes compared to the vesicles in a methanol solution. Interestingly, both the addition of methanol and in particular the peptides, increased the activation energy for flip-flop that is compensated by entropic factors that lead to more rapid process overall.

More recently, TR-SANS was used to isolate and study lipid flip-flop in asymmetric vesicles with protoeated and deuterated lipids on the inner and outer leaflets respectively. The vesicles are prepared using a protocol involving cyclodextrin to facilitate selective exchange of lipids at the outer leaflet. Using this technique Nguyen *et al.* found consistently faster kinetics for POPC by addition of the AMPs, melittin and alamethicin dissolved in small volume of methanol [82]. POPC with a C18 tail show exceedingly slow flip-flop rates but with addition of peptides, the half time, $t_{1/2}$, decreased from about 140 h to a few hours. Similarly Marx *et al.* studied mixed POPE/POPG ULVs which were mixed with various amounts of the AMPs; frog sourced peptides L18W-PGLa and magainin II, as well as the lactoferricin derivative LF11-215 in a buffer solution [83]. They found that L18W-PGLa caused the strongest effect with significant faster flip-flop rates, while magainin II cause less dramatic effects in a manner correlated with their membrane partition. On the other hand, LF11-215, which has the highest antibacterial activity (lowest MIC), caused essentially no change in the lipid dynamics despite that it is found to be able to translocate through the bacterial envelope of *E. coli.* This suggests that the ability to cause flip-flop and translocation through membranes are not necessary correlated.

In a study, Nielsen *et al.* investigated the combined lipid dynamics and structural evolution following the TR-SAXS data over the whole Q range after exposure of AMPs [49]. It was found, using both dynamic light scattering (DLS) and TR-SANS, that AMPs lead to a concurrent increase in the vesicle size which was attributed to an enhanced Ostwald ripening-like effect which occurred during an initial homogenisation process while the peptides are redistributed between vesicles after a rapid ~ms insertion. Comparing the kinetics of pre-inserted peptides, that is, when the AMPs are incubated with the labelled vesicles prior to mixing, it was shown that after pre-equilibration the kinetics is slightly slower but the two processes can be deconvoluted if the whole time dependent scattering curves are analysed. This study showed that care must be taken in the analysis of TR-SANS when structural relaxation occurs in parallel with lipid exchange processes.

Taken together, the results of the effect of AMP on the lipid dynamics are rather intriguing as it shows even weakly interacting and non-penetrating (non-transmembrane) peptides may have a rather dramatic effect. This brings into discussion the mode of action of AMPs and whether pores in the classical sense are necessary to compromise the integrity of the cell. Disordering the lipid packing and acceleration of flip-flop kinetics might lead to scrambling of lipid compositions, transient pores and enhanced ion transport at physiologically relevant concentrations.

Conclusion and outlook

The aim of this short review is to give an overview of studies on peptide-lipid membrane interactions focussing specifically on the level of information that can be extracted using small-angle scattering techniques. Using model lipid membranes, specifically well-defined unilamellar vesicles, X-rays combined with advanced data modelling, give unique insight into insertion and spatial distribution of peptides within the membranes. Neutron techniques are on the other hand able to isolate individual components using contrast variation, and monitor kinetic processes associated with the transport of lipids and potentially other biomolecules. A limitation, as well as the strength of these techniques, is related to the ensemble average, that is, the experiments average over very large number of particles in the scattering volume, which creates challenges for heterogeneous, ill-defined and complicated mixtures of structures. This can, for example, occur when peptides solubilise parts of the vesicle and create new (meta) stable mesophases. Complementary methods are important, in particular cryo-TEM is useful in mapping structural pathways and in pin-pointing complex structures [84], while DLS and/or Nanoparticle tracking analysis can provide information on size changes and distribution of sizes outside of the Q-range of SAS. Zeta-potential measurements ("Zetasizers") can provide information on the changes in the surface charge of the vesicles upon peptide insertion. Computer simulations techniques are also essential for understanding the interplay of interactions, structure and kinetic pathways in self-assembled systems including lipid membranes. Advances in coarse-graining methods combined with SAXS/SANS biased simulations offer exciting

possibilities to study large systems/long time scales that give new unique insight into rather complex processes and mechanisms in these systems [85].These advances will also help to understand dynamic properties, for example, lipid flip-flop and membrane fluctuations and elucidate the mechanism for transient pore-formation facilitating ion transport.

With new advances in instrumentation and powerful sources such as spallation and free electron/synchrotron sources, a new window of opportunity is opened where extremely fast processes and small sample volumes with low concentrations can be probed reliably. In combination with imaging techniques such as coherent X-ray and electron microscopy techniques, scattering techniques are expected to be increasingly used to get detailed insight into "real" biological systems such as living cells and microorganisms. So far only live bacteria have been probed by SAS, but in the future also peptide effect on virus envelopes or parasite membranes using real cells could be studied by SAS, providing new information on potential targets for drugs. Neutron scattering with contrast variation schemes through genetic and chemical manipulation of the live organisms, has already been shown to be able to detect subtle structural details such as membrane domains (rafts) in living bacteria [9]. With more advanced biochemical techniques that allow for selective deuteration, neutron scattering will allow for more targeted investigation of the mechanism of peptide based drugs on micro-organisms.

In conclusion, advances in X-ray/neutron techniques combined with quantitative analysis, including computer simulations lead the way to deeper understanding of complex interactions in membrane systems that will be crucial for new drug and vaccine design as well as molecular understanding of many diseases.

Declaration of competing interest

The authors declare that they have no known competing financial interests or personal relationships that could have appeared to influence the work reported in this paper.

Data availability

Data will be made available on request.

Acknowledgement

The authors gratefully acknowledge funding from the Norwegian Research Council (Project no. 315666) and NordForsk (Project no. 82004) for financial support.

References

Papers of particular interest, published within the period of review, have been highlighted as:

* of special interest
** of outstanding interest

1. Sparr E, Linse S: **Lipid-protein interactions in amyloid formation**. *Biochim Biophys Acta Proteins Proteom* 2019, **1867**: 455–457, https://doi.org/10.1016/j.bbapap.2019.03.006.

2. Brogden KA: **Antimicrobial peptides: pore formers or metabolic inhibitors in bacteria?** *Nat Rev Microbiol* 2005, **3**: 238–250, https://doi.org/10.1038/nrmicro1098.

3. Zhang L, Rozek A, Hancock RE: **Interaction of cationic antimicrobial peptides with model membranes**. *J Biol Chem* 2001, **276**:35714–35722, https://doi.org/10.1074/jbc.m104925200.

4. Lund R, Willner L, Richter D: **Kinetics of block copolymer micelles studied by small-angle scattering methods**. In *Controlled polymerization and polymeric structures*. Edited by Abe A, Lee K-S, Leibler L, Kobayashi S, Cham: Springer; 2013: 51–158.

5. Narayanan T, Wacklin H, Konovalov O, Lund R: **Recent applications of synchrotron radiation and neutrons in the study of soft matter**. *Crystallogr Rev* 2017, **23**:160–226, https://doi.org/10.1080/0889311X.2016.1277212.

6. **Neutron, X-rays and light**. In *Scattering methods applied to soft condensed matter*. Edited by Zemb T, Lindner P, Oxford, England: North-Holland Delta S., North-Holland; 2002.

7. Perez-Salas U, Garg S, Gerelli Y, Porcar L: **Deciphering lipid transfer between and within membranes with time-resolved small-angle neutron scattering**. In *New methods and sensors for membrane and cell volume Research*. Elsevier; 2021: 359–412, https://doi.org/10.1016/bs.ctm.2021.10.004.

8. Semeraro EF, Devos JM, Porcar L, Forsyth VT, Narayanan T: **In vivo analysis of the Escherichia coli ultrastructure by small-angle scattering**. *IUCrJ* 2017, **4**:751–757, https://doi.org/10.1107/S2052252517013008.

9. Nickels JD, Chatterjee S, Stanley CB, Qian S, Cheng X, Myles DA, Standaert RF, Elkins JG, Katsaras J: **The in vivo structure of biological membranes and evidence for lipid domains**. *PLoS Biol* 2017, **15**, e2002214, https://doi.org/10.1371/journal.pbio.2002214.

10. ** Malanovic N, Marx L, Blondelle SE, Pabst G, Semeraro EF: **Experimental concepts for linking the biological activities of antimicrobial peptides to their molecular modes of action**. *Biochim Biophys Acta Biomembr* 2020, **1862**, 183275, https://doi.org/10.1016/j.bbamem.2020.183275.
A comprehensive and critical review of the different experimental methods used to study antimicrobial peptides, focussing on the comparison between live bacterial studies and lipid model membranes.

11. * Clifton LA, Campbell RA, Sebastiani F, Campos-Terán J, Gonzalez-Martinez JF, Björklund S, Sotres J, Cárdenas M: **Design and use of model membranes to study biomolecular interactions using complementary surface-sensitive techniques**. *Adv Colloid Interface Sci* 2020, **277**, 102118, https://doi.org/10.1016/j.cis.2020.102118.
A thorough review on the preparation of planar model membranes and the use of different surface sensitive techniques to study the molecular interactions between membranes and various biomolecules, including antimicrobial peptides.

12. Marquardt D, Geier B, Pabst G: **Asymmetric lipid membranes: towards more realistic model systems**. *Membranes* 2015, **5**: 180–196, https://doi.org/10.3390/membranes5020180.

13. Scott HL, Kennison KB, Enoki TA, Doktorova M, Kinnun JJ, Heberle FA, Katsaras J: **Model membrane systems used to study plasma membrane lipid asymmetry**. *Symmetry* 2021, **13**: 1356, https://doi.org/10.3390/sym13081356.

14. Hirai M, Iwase H, Hayakawa T, Koizumi M, Takahashi H: **Determination of asymmetric structure of ganglioside-DPPC mixed vesicle using SANS, SAXS, and DLS**. *Biophys J* 2003, **85**: 1600–1610, https://doi.org/10.1016/s0006-3495(03)74591-3.

15. Pencer J, Krueger S, Adams CP, Katsaras J: **Method of separated form factors for polydisperse vesicles**. *J Appl Crystallogr* 2006, **39**:293–303, https://doi.org/10.1107/S0021889806005255.

16. Qian S, Heller WT: **Peptide-induced asymmetric distribution of charged lipids in a vesicle bilayer revealed by small-angle neutron scattering**. *J Phys Chem B* 2011, **115**:9831–9837, https://doi.org/10.1021/jp204045t.

17. Rai DK, Sharma VK, Anunciado D, O'Neill H, Mamontov E, Urban V, Heller WT, Qian S: **Neutron scattering studies of the interplay of amyloid β peptide(1-40) and an anionic lipid 1,2-dimyristoyl-sn-glycero-3-phosphoglycerol**. *Sci Rep* 2016, **6**, 30983, https://doi.org/10.1038/srep30983.

18. Bjørnestad VA, Orwick-Rydmark M, Lund R: **Understanding the structural pathways for lipid nanodisc formation: how styrene maleic acid copolymers induce membrane fracture and disc formation**. *Langmuir* 2021, **37**:6178–6188, https://doi.org/10.1021/acs.langmuir.1c00304.

19. Kučerka N, Kiselev MA, Balgavý P: **Determination of bilayer thickness and lipid surface area in unilamellar dimyristoylphosphatidylcholine vesicles from small-angle neutron scattering curves: a comparison of evaluation methods**. *Eur Biophys J* 2003, **33**:328–334, https://doi.org/10.1007/s00249-003-0349-0.

20. Brzustowicz MR, Brunger AT: **X-ray scattering from unilamellar lipid vesicles**. *J Appl Crystallogr* 2005, **38**:126–131, https://doi.org/10.1107/S0021889804029206.

21. Kučerka N, Pencer J, Sachs JN, Nagle JF, Katsaras J: **Curvature effect on the structure of phospholipid bilayers**. *Langmuir* 2007, **23**:1292–1299, https://doi.org/10.1021/la062455t.

22. ** Eicher B, Heberle FA, Marquardt D, Rechberger GN, Katsaras J, Pabst G: **Joint small-angle X-ray and neutron scattering data analysis of asymmetric lipid vesicles**. *J Appl Crystallogr* 2017, **50**, https://doi.org/10.1107/S1600576717000656.
A comprehensive overview of the SDP model, and its use in joint analysis of SAXS/SANS data from asymmetric lipid vesicles, compared to simpler slab models.

23. * Kinnun JJ, Scott HL, Ashkar R, Katsaras J: **Biomembrane structure and material properties studied with neutron scattering**. *Front Chem* 2021, **9**, https://doi.org/10.3389/fchem.2021.642851.
A thorough review on the use and unique advantages presented by different neutron scattering techniques in the study of lipid membranes, and the insights they have facilitated.

24. ** Nielsen JE, Bjørnestad VA, Lund R: **Resolving the structural interactions between antimicrobial peptides and lipid membranes using small-angle scattering methods: the case of indolicidin**. *Soft Matter* 2018, **14**:8750–8763, https://doi.org/10.1039/C8SM01888J.
Describes how the peptide- membrane interaction can be resolved structurally using detailed quantitative modelling of SAXS data on an absolute scale based on the SDP model.

25. Jacques DA, Guss JM, Svergun DI, Trewhella J: **Publication guidelines for structural modelling of small-angle scattering data from biomolecules in solution**. *Acta Crystallogr Sect D Biol Crystallogr* 2012, **68**:620–626, https://doi.org/10.1107/s0907444912012073.

26. Franke D, Jeffries CM, Svergun DI: **Correlation Map, a goodness-of-fit test for one-dimensional X-ray scattering spectra**. *Nat Methods* 2015, **12**:419–422, https://doi.org/10.1038/nmeth.3358.

27. Pedersen JS: **Small-angle scattering from surfactants and block copolymer micelles**. In *Soft matter characterization*. Springer Netherlands; 2008:191–233, https://doi.org/10.1007/978-1-4020-4465-6_4.

28. Chappa V, Smirnova Y, Komorowski K, Müller M, Salditt T: **The effect of polydispersity, shape fluctuations and curvature on small unilamellar vesicle small-angle X-ray scattering curves**. *J Appl Crystallogr* 2021, **54**(Pt 2):557–568, https://doi.org/10.1107/S1600576721001461.

29. ** Nielsen JE, Bjørnestad VA, Pipich V, Jenssen H, Lund R: **Beyond structural models for the mode of action: how natural antimicrobial peptides disrupts lipid membranes**. *J Colloid Interface Sci* 2021, **582**:793–802, https://doi.org/10.1016/j.jcis.2020.08.094.
Systematic study on a number of natural surface active peptides, comparing their structural interactions with model lipid membranes as seen by SAXS, with their effect on lipid dynamics as seen by time resolved SANS.

30. Kiselev M, Lesieur P, Kisselev A, Lombardo D, Aksenov V: **Model of separated form factors for unilamellar vesicles**. *Appl Phys A* 2002, **74**:s1654–s1656, https://doi.org/10.1007/s003390201837.

31. Kučerka N, Nagle JF, Sachs JN, Feller SE, Pencer J, Jackson A, Katsaras J: **Lipid bilayer structure determined by the simultaneous analysis of neutron and X-ray scattering data**. *Biophys J* 2008, **95**:2356–2367, https://doi.org/10.1529/biophysj.108.132662.

32. Klauda JB, Kučerka N, Brooks BR, Pastor RW, Nagle JF: **Simulation-based methods for interpreting X-ray data from lipid bilayers**. *Biophys J* 2006, **90**:2796–2807, https://doi.org/10.1529/biophysj.105.075697.

33. Pan J, Heberle FA, Tristram-Nagle S, Szymanski M, Koepfinger M, Katsaras J, Kučerka N: **Molecular structures of fluid phase phosphatidylglycerol bilayers as determined by small angle neutron and X-ray scattering**. *Biochim Biophys Acta Biomembr* 2012, **1818**:2135–2148, https://doi.org/10.1016/j.bbamem.2012.05.007.

34. Nagle JF, Venable RM, Maroclo-Kemmerling E, Tristram-Nagle S, Harper PE, Pastor RW: **Revisiting volumes of lipid components in bilayers**. *J Phys Chem B* 2019, **123**:2697–2709, https://doi.org/10.1021/acs.jpcb.8b12010. publisher: American Chemical Society.

35. Brodszkij E, Westensee IN, Holleufer SF, Ade C, Andres PDD, Pedersen JS, Städler B: **Membrane composition of polymer-lipid hybrid vesicles**. *Appl Mater Today* 2022, **29**, 101549, https://doi.org/10.1016/j.apmt.2022.101549.

36. Sevcsik E, Pabst G, Jilek A, Lohner K: **How lipids influence the mode of action of membrane-active peptides**. *Biochim Biophys Acta, Biomembr* 2007, **1768**:2586–2595, https://doi.org/10.1016/j.bbamem.2007.06.015.

37. Sevcsik E, Pabst G, Richter W, Danner S, Amenitsch H, Lohner K: **Interaction of LL-37 with model membrane systems of different complexity: influence of the lipid matrix**. *Biophys J* 2008, **94**:4688–4699, https://doi.org/10.1529/biophysj.107.123620.

38. Galvagnion C, Barclay A, Makasewicz K, Marlet FR, Moulin M, Devos J, Linse S, Martel A, Porcar L, Sparr E, Pedersen MC, Roosen-Runge F, Arleth L, Büll AK: *Structural characterisation of α-synuclein-membrane interactions and the resulting aggregation using small angle scattering*. 2023, https://doi.org/10.26434/chemrxiv-2023-6hsh2.

39. ** Semeraro EF, Marx L, Mandl J, Letofsky-Papst I, Mayrhofer C, Frewein MP, Scott HL, Prévost S, Bergler H, Lohner K, *et al.*: **Lactoferricins impair the cytosolic membrane of *Escherichia coli* within a few seconds and accumulate inside the cell**. *Elife* 2022, **11**, e72850, https://doi.org/10.7554/eLife.72850.
First study to show the real-time response of real bacterial cells to an antimicrobial peptide, showing how information on the peptide information can be gained by careful analysis of SAS data even in real cells.

40. Kabelka I, Georgiev V, Marx L, Pajtinka P, Lohner K, Pabst G, Dimova R, Vácha R: **Magainin 2 and PGLa in bacterial membrane mimics III: membrane fusion and disruption**. *Biophys J* 2022, **121**:852–861, https://doi.org/10.1016/j.bpj.2021.12.035.

41. Nielsen JE, Prévost SF, Jenssen H, Lund R: **Impact of antimicrobial peptides on *E. coli*-mimicking lipid model membranes: correlating structural and dynamic effects using scattering methods**. *Faraday Discuss* 2021, **232**:203–217, https://doi.org/10.1039/D0FD00046A.

42. Freire RV, Pillco-Valencia Y, da Hora GC, Ramstedt M, Sandblad L, Soares TA, Salentinig S: **Antimicrobial peptide induced colloidal transformations in bacteria-mimetic vesicles: combining in silico tools and experimental methods**. *J Colloid Interface Sci* 2021, **596**:352–363, https://doi.org/10.1016/j.jcis.2021.03.060.

43. Wimley WC: **Describing the mechanism of antimicrobial peptide action with the interfacial activity model**. *ACS Chem Biol* 2010, **5**:905–917, https://doi.org/10.1021/cb1001558.

44. Chongsiriwatana NP, Lin JS, Kapoor R, Wetzler M, Rea JA, Didwania MK, Contag CH, Barron AE: **Intracellular biomass flocculation as a key mechanism of rapid bacterial killing by cationic, amphipathic antimicrobial peptides and peptoids**.

Sci Rep 2017, **7**:1–15, https://doi.org/10.1038/s41598-017-16180-0.

45. Nielsen JE, Lind TK, Lone A, Gerelli Y, Hansen PR, Jenssen H, Cárdenas M, Lund R: **A biophysical study of the interactions between the antimicrobial peptide indolicidin and lipid model systems**. *Biochim Biophys Acta, Biomembr* 2019, **1861**: 1355–1364, https://doi.org/10.1016/j.bbamem.2019.04.003.

46. Schmidt NW, Mishra A, Lai GH, Davis M, Sanders LK, Tran D, Garcia A, Tai KP, McCray PB, Ouellette AJ, Selsted ME, Wong GCL: **Criterion for amino acid composition of defensins and antimicrobial peptides based on geometry of membrane destabilization**. *J Am Chem Soc* 2011, **133**:6720–6727, https://doi.org/10.1021/ja200079a.

47. Pabst G, Grage SL, Danner-Pongratz S, Jing W, Ulrich AS, Watts A, Lohner K, Hickel A: **Membrane thickening by the antimicrobial peptide PGLa**. *Biophys J* 2008, **95**:5779–5788, https://doi.org/10.1529/biophysj.108.141630.

48. * Pachler M, Kabelka I, Appavou M-S, Lohner K, Vácha R, Pabst G: **Magainin 2 and PGLa in bacterial membrane mimics I: peptide-peptide and lipid-peptide interactions**. *Biophys J* 2019, **117**:1858–1869, https://doi.org/10.1016/j.bpj.2019.10.022.
Describing the power of a combined MD simulation and SAS based approach to studying the peptide-lipid interactions.

49. Nielsen JE, Lund R: **Molecular transport and growth of lipid vesicles exposed to antimicrobial peptides**. *Langmuir* 2021, **38**:374–384, https://doi.org/10.1021/acs.langmuir.1c02736.

50. Hristova K, Dempsey CE, White SH: **Structure, location, and lipid perturbations of melittin at the membrane interface**. *Biophys J* 2001, **80**:801–811, https://doi.org/10.1016/s0006-3495(01)76059-6.

51. Lee M-T, Sun T-L, Hung W-C, Huang HW: **Process of inducing pores in membranes by melittin**. *Proc Natl Acad Sci USA* 2013, **110**:14243–14248, https://doi.org/10.1073/pnas.1307010110.

52. Dupuy FG, Pagano I, Andenoro K, Peralta MF, Elhady Y, Heinrich F, Tristram-Nagle S: **Selective interaction of colistin with lipid model membranes**. *Biophys J* 2018, **114**:919–928, https://doi.org/10.1016/j.bpj.2017.12.027.

53. Castelletto V, Barnes RH, Karatzas K-A, Edwards-Gayle CJ, Greco F, Hamley IW, Seitsonen J, Ruokolainen J: **Restructuring of lipid membranes by an arginine-capped peptide bolaamphiphile**. *Langmuir* 2019, https://doi.org/10.1021/acs.langmuir.8b01014.

54. Castelletto V, Barnes RH, Karatzas K-A, Edwards-Gayle CJ, Greco F, Hamley IW, Rambo R, Seitsonen J, Ruokolainen J: **Arginine-containing surfactant-like peptides: interaction with lipid membranes and antimicrobial activity**. *Biomacromolecules* 2018, https://doi.org/10.1021/acs.biomac.8b00391.

55. Edwards-Gayle CJC, Barrett G, Roy S, Castelletto V, Seitsonen J, Ruokolainen J, Hamley IW: **Selective antibacterial activity and lipid membrane interactions of arginine-rich amphiphilic peptides**. *ACS Appl Bio Mater* 2020, **3**:1165–1175, https://doi.org/10.1021/acsabm.9b00894.

56. Lone A, Thomsen TT, Nielsen JE, Thulstrup PW, Klitgaard RN, Løbner-Olesen A, Lund R, Jenssen H, Hansen PR: **Structure-activity study of an all-d antimicrobial octapeptide D2D**. *Molecules* 2019, **24**:4571, https://doi.org/10.3390/molecules24244571.

57. Heinrich F, Salyapongse A, Kumagai A, Dupuy FG, Shukla K, Penk A, Huster D, Ernst RK, Pavlova A, Gumbart JC, Deslouches B, Di YP, Tristram-Nagle S: **Synergistic biophysical techniques reveal structural mechanisms of engineered cationic antimicrobial peptides in lipid model membranes**. *Chemistry* 2020, **26**: 6247–6256, https://doi.org/10.1002/chem.202000212.

58. Lone A, Nielsen JE, Thulstrup PW, Lund R, Hansen PR, Jenssen H: **Cyclic N-locked indolicidin analogues with antimicrobial activity: effect of ring size and fatty acid acylation**. *Eur J Med Chem Rep* 2022, **6**, 100080, https://doi.org/10.1016/j.ejmcr.2022.100080.

59. Xu D, Jiang L, Singh A, Dustin D, Yang M, Liu L, Lund R, Sellati TJ, Dong H: **Designed supramolecular filamentous peptides: balance of nanostructure, cytotoxicity and antimicrobial activity**. *Chem Commun* 2015, **51**:1289–1292, https://doi.org/10.1039/c4cc08808e.

60. Nielsen JE, König N, Yang S, Skoda MWA, Maestro A, Dong H, Cárdenas M, Lund R: **Lipid membrane interactions of self-assembling antimicrobial nanofibers: effect of PEGylation**. *RSC Adv* 2020, **10**:35329–35340, https://doi.org/10.1039/D0RA07679A.

61. von Gundlach A, Ashby MP, Gani J, Lopez-Perez PM, Cookson AR, Huws SA, Rumancev C, Garamus VM, Mikut R, Rosenhahn A, Hilpert K: **BioSAXS measurements reveal that two antimicrobial peptides induce similar molecular changes in gram-negative and gram-positive bacteria**. *Front Pharmacol* 2019, **10**, https://doi.org/10.3389/fphar.2019.01127.

62. Ivankov O, Murugova TN, Ermakova EV, Kondela T, Badreeva DR, Hrubovčák P, Soloviov D, Tsarenko A, Rogachev A, Kuklin AI, Kučerka N: **Amyloid-beta peptide (25-35) triggers a reorganization of lipid membranes driven by temperature changes**. *Sci Rep* 2021, **11**, 21990, https://doi.org/10.1038/s41598-021-01347-7.

63. Ulmer TS, Bax A, Cole NB, Nussbaum RL: **Structure and dynamics of micelle-bound human α-synuclein**. *J Biol Chem* 2005, **280**:9595–9603, https://doi.org/10.1074/jbc.M411805200.

64. * Dubackic M, Liu Y, Kelley EG, Hetherington C, Haertlein M, Devos JM, Linse S, Sparr E, Olsson U: **α-Synuclein interaction with lipid bilayer discs**. *Langmuir* 2022, **38**:10216–10224, https://doi.org/10.1021/acs.langmuir.2c01368.
Shows how contrast-matching and SANS can be used to study the effect of adding self-assembling peptides, in this case partly deuterated α-synuclein, to the structure, herunder morphology of lipid model membranes

65. Carrotta R, Mangione MR, Librizzi F, Moran O: **Small angle X-ray scattering sensing membrane composition: the role of sphingolipids in membrane-amyloid β-peptide interaction**. *Biology* 2021, **11**:26, https://doi.org/10.3390/biology11010026.

66. Dubackic M, Linse S, Sparr E, Olsson U: **Comparing α-synuclein fibrils formed in the absence and presence of a model lipid membrane: a small and wide-angle X-ray scattering study**. *Front Soft Matter* 2022, **1**, https://doi.org/10.3389/frsfm.2021.741996.

67. Pallbo J, Imai M, Gentile L, Takata S-I, Olsson U, Sparr E: **NACore amyloid formation in the presence of phospholipids**. *Front Physiol* 2020, **11**, 592117, https://doi.org/10.3389/fphys.2020.592117.

68. Martel A, Antony L, Gerelli Y, Porcar L, Fluitt A, Hoffmann K, Kiesel I, Vivaudou M, Fragneto G, de Pablo JJ: **Membrane permeation versus amyloidogenicity: a multitechnique study of islet amyloid polypeptide interaction with model membranes**. *J Am Chem Soc* 2017, **139**:137–148, https://doi.org/10.1021/jacs.6b06985.

69. Gerbelli BB, Oliveira CLP, Silva ER, Hamley IW, Alves WA: **Amyloid Formation by short peptides in the presence of dipalmitoylphosphatidylcholine membranes**. *Langmuir* 2020, **36**:14793–14801, https://doi.org/10.1021/acs.langmuir.0c02760.

70. Narayanan T, Weerakkody D, Karabadzhak AG, Anderson M, Andreev OA, Reshetnyak YK: **pHLIP peptide interaction with a membrane monitored by SAXS**. *J Phys Chem B* 2016, **120**: 11484–11491, https://doi.org/10.1021/acs.jpcb.6b06643. publisher: American Chemical Society.

71. Sharma VK, Mamontov E: **Multiscale lipid membrane dynamics as revealed by neutron spectroscopy**. *Prog Lipid Res* 2022, **87**, 101179, https://doi.org/10.1016/j.plipres.2022.101179.

72. * Hong L, Gontsarik M, Amenitsch H, Salentinig S: **Human antimicrobial peptide triggered colloidal transformations in bacteria membrane lipopolysaccharides**. *Small* 2021, **18**, 2104211, https://doi.org/10.1002/smll.202104211.
A study of structural transformations in lipopolysaccharide membranes upon addition of the human cathelicidin, LL37.

73. Bjørnestad VA, Lund R: **Pathways of membrane solubilization: a structural study of model lipid vesicles exposed to classical detergents**. *Langmuir* 2023, **39**:3914–3933, https://doi.org/10.1021/acs.langmuir.2c03207.

74. Jensen GV, Lund R, Gummel J, Narayanan T, Pedersen JS: **Monitoring the transition from spherical to polymer-like surfactant micelles using small-angle X-ray scattering**. *Angew Chem Int Ed* 2014, **53**:11524–11528, https://doi.org/10.1002/ange.201406489.

75. Varga Z, Wacha A, Bóta A: **Osmotic shrinkage of sterically stabilized liposomes as revealed by time-resolved small-angle X-ray scattering**. *J Appl Crystallogr* 2014, **47**:35–40, https://doi.org/10.1107/s1600576713030513.

76. Marx L, Semeraro EF, Mandl J, Kremser J, Frewein MP, Malanovic N, Lohner K, Pabst G: **Bridging the antimicrobial activity of two lactoferricin derivatives in *E. coli* and lipid-only membranes**. *Front Med Technol* 2021, **3**, https://doi.org/10.3389/fmedt.2021.625975.

77. * Nakano M, Fukuda M, Kudo T, Endo H, Handa T: **Determination of interbilayer and transbilayer lipid Transfers by time-resolved small-angle neutron scattering**. *Phys Rev Lett* 2007, **98**:2628, https://doi.org/10.1103/PhysRevLett.98.238101. 4.
First study of the kinetics of lipid flip-flop and exchange processes in vesicles using time-resolved SANS and contrast variation.

78. Nakano M, Fukuda M, Kudo T, Matsuzaki N, Azuma T, Sekine K, Endo H, Handa T: **Flip-flop of phospholipids in vesicles: kinetic analysis with time-resolved small-angle neutron scattering**. *J Phys Chem B* 2009, **113**:6745–6748, https://doi.org/10.1021/jp900913w.

79. Lund R, Willner L, Pipich V, Grillo I, Lindner P, Colmenero J, Richter D: **Equilibrium chain exchange kinetics of diblock copolymer micelles: effect of morphology**. *Macromolecules* 2011, **44**:6145–6154, https://doi.org/10.1021/ma200532r.

80. Garg S, Porcar L, Woodka A, Butler P, Perez-Salas U: **Noninvasive neutron scattering measurements reveal slower cholesterol transport in model lipid membranes**. *Biophys J* 2011, **101**:370–377, https://doi.org/10.1016/j.bpj.2011.06.014.

81. Khondker A, Rheinstädter MC: **How do bacterial membranes resist polymyxin antibiotics?** *Commun Biol* 2020, **3**:1–4, https://doi.org/10.1038/s42003-020-0803-x. number: 1 Publisher: Nature Publishing Group.

82. ** Nguyen MHL, DiPasquale M, Rickeard BW, Doktorova M, Heberle FA, Scott HL, Barrera FN, Taylor G, Collier CP, Stanley CB, Katsaras J, Marquardt D: **Peptide-induced lipid flip-flop in asymmetric liposomes measured by small angle neutron scattering**. *Langmuir* 2019, **35**:11735–11744, https://doi.org/10.1021/acs.langmuir.9b01625.
A study of the influence of AMPs om lipid flip-flop introducing a novel concept of asymmetrically labelled vesicles.

83. * Marx L, Frewein MPK, Semeraro EF, Rechberger GN, Lohner K, Porcar L, Pabst G: **Antimicrobial peptide activity in asymmetric bacterial membrane mimics**. *Faraday Discuss* 2021, **232**:435–447, https://doi.org/10.1039/d1fd00039j.
A study combining various techniques to correlate peptide partitioning and translocation with the flip-flop lipid kinetics in asymmetric membranes

84. Bjørnestad VA, Soto-Bustamante F, Tria G, Laurati M, Lund R: **Beyond the standard model of solubilization: non-ionic surfactants induce collapse of lipid vesicles into rippled bilamellar nanodiscs**. *J Colloid Interface Sci* 2023, **641**:553–567, https://doi.org/10.1016/j.jcis.2023.03.037.

85. Chatzimagas L, Hub JS: *Predicting solution scattering patterns with explicit-solvent molecular simulations*. 2022, https://doi.org/10.48550/ARXIV.2204.04961.